*ANZIAM J.* **65** (2023), 111–134
doi:10.1017/S144618112300007X

# MODELLING MICROWAVES IN BAUXITE

LATA I. PAEA[1], SIONE PAEA[1] and MARK J. MCGUINNESS[✉2]

(Received 2 January, 2023; accepted 3 March, 2023; first published online 4 July, 2023)

**Abstract**

Sending microwaves through bauxite ore allows almost continuous measurement of moisture content during offload by conveyor belt from a ship. Data and results from a microwave analyser were brought to a European Study Group with Industry at the University of Limerick, with the over-arching question of whether the results are accurate enough. The analyser equipment uses linear regression against phase shifts and signal attenuation to infer moisture content in real time. Simple initial modelling conducted during the Study Group supports this use of linear regression for phase shift data. However, that work also revealed striking and puzzling differences between model and attenuation data.

We present an improved model that allows for multiple reflections of travelling microwaves within the bauxite and in the air above it. Our new model uses four differential equations to describe how electric fields change with distance in each of four layers. By solving these equations and taking reflections into account, we can accurately predict what the receiving antenna will pick up.

Our new solution provides much-improved matches to data from the microwave analyser, and indicates the deleterious effects of reflections. Modelled signal strength behaviour features a highly undesirable noninvertible dependence on bauxite mixture permittivity.

Practical measures that might be expected to reduce the effects of microwave reflections and improve the accuracy of microwave analyser results are suggested based on our improved model solution. This modelling approach and these results are anticipated to extend to the analysis of moisture content during transport on conveyor belts of other ores, slurries, coal, grains and pharmaceutical powders, especially when the depth of the conveyed material is variable.

2020 *Mathematics subject classification*: primary 78-10; secondary 78-02.

*Keywords and phrases*: mathematics in industry, modelling with differential equations, automated detection of moisture in bauxite, travelling waves, reflections, interference.

[1]School of Information Technology, Engineering, Mathematics and Physics, The University of the South Pacific, Suva, Fiji; e-mail: s11148975@student.usp.ac.fj, sione.paea@usp.ac.fj
[2]School of Mathematics and Statistics, Victoria University of Wellington, Wellington, New Zealand; e-mail: Mark.McGuinness@vuw.ac.nz

*The European Study Group with Industry that motivated the work in this manuscript is one of many such that Graeme Hocking regularly attends, in Limerick and around the world, often as Moderator, and always as an enthusiastic expert. We are pleased to be able to contribute this research paper to a special edition honouring Professor Hocking's significant global contributions to industrial mathematics over many years.*

## 1. Introduction

The use of low-powered microwaves to automatically detect moisture content of powder or bulk solids in real time on a conveyor belt is key for the pricing and control of a number of industrial processes, including ore, coal, bauxite, grains, seeds, pelleted biomass and pharmaceuticals. However, the technology in use does not always reflect a good understanding of the effects of varying setups and conditions on analyser reliability.

We present an example of microwave use in the bauxite industry, and show how it benefits from the improved understanding that applied mathematics provides. Our example comes from a challenge that was brought to the 128th European Study Group with Industry (ESGI) in 2017 at the University of Limerick in Ireland. Bauxite electromagnetic measurements taken by an automatic microwave analyser during offload from a ship to an alumina factory were provided to the Study Group, and have provided the guiding impetus for our modelling efforts. The measurements show that while phase shift data from the analyser provide a useful indication of moisture content, signal attenuation data do not look helpful [12]. The algorithms used in the analyser are based on linear regression models using both signal strength and phase shift. However, the signal attenuation recorded by the analyser and reported by McGuinness et al. [12] is strongly nonlinear when plotted against bauxite height (depth). It has been speculated [12] that internal reflections and wave interference might account for the highly oscillatory behaviour seen in attenuation data from the analyser.

This effect of reflections of microwaves is avoided in applications where measurements are taken across material flowing down a circular cross-section, so that the average thickness of the material is constant and there is a curved interface between material and air. Then thickness can be ignored, while density variations have a significant effect on measurements and moisture content inference [15].

We present a new mathematical model of microwave travel through a layer of bauxite with air gaps above and below. The meaning of the word model is broad, and in [21], for example, it is applied to the use of a simple linear regression model to infer bauxite moisture content. Moisture content is taken to be proportional to phase shift divided by total mass, and to attenuation divided by total mass. Density and height (depth) of bauxite both affect total mass, which may also be measured directly on a conveyor belt. However, Viana [21] found that using belt tonnage scales to measure mass led to unreliable and inaccurate analyser values for moisture content, when using the analyser in an alumina plant in Brazil. Instead, they obtained more reliable results if

https://doi.org/10.1017/S144618112300007X Published online by Cambridge University Press

they used measurements of material height instead of mass, thereby assuming constant material porosity.

Viana [21] uses the same regression formula as the one used in the microwave analyser that provided our data from the ESGI, in which the moisture content $M$ (mass of water per unit mass of moist bauxite mixture) is given by

$$M = c_0 + c_1 \frac{\Delta\phi}{h} + c_2 \frac{L}{h}, \tag{1.1}$$

where the constants $c_0$, $c_1$ and $c_2$ are fitted during calibration to the moisture content of laboratory samples, $\Delta\phi$ is the phase shift (radians) in the complex valued electric field $E(h)$ signal at the receiving antenna when bauxite height is $h$, and $L$ is the signal attenuation, given in dB by

$$L = -20 \log_{10} \left| \frac{E(h)}{E(0)} \right|. \tag{1.2}$$

This form for attenuation is also referred to as the electromagnetic shielding efficiency [22] of the bauxite material. The phase shift is the difference in radians between the phase or argument of the complex number $E(h)$ and the phase or argument of $E(0)$ (recorded when the conveyor belt is empty).

Such a simple model is noted to require careful and frequent calibration of the analyser [21], and careful treatment of the lab samples used to calibrate. Special care is needed to ensure that sample times match analyser times [12].

Rearranging the regression formula (1.1) and assuming constant moisture content then requires that phase shift divided by $h$ is constant, and that attenuation divided by $h$ is constant. That is, if moisture content does not change much, then phase shift and attenuation must both be proportional to or linear in $h$. There is some support in Figure 1 for measured phase shifts being linear in bauxite height, but it is clear that attenuation is highly oscillatory and a linear approximation is going to perform poorly [12].

**1.1. Maxwell's equations** The regression formula (1.1) used by the microwave analyser may be justified by considering a more sophisticated kind of model for microwave propagation in bauxite. Maxwell's equations for electromagnetic propagation in a stationary linear isotropic conducting dielectric material may be written in the form [10]

$$\nabla \cdot \mathbf{E} = \rho_f / \epsilon, \tag{1.3a}$$

$$\nabla \cdot \mathbf{B} = 0, \tag{1.3b}$$

$$\nabla \times \mathbf{E} = -\frac{\partial \mathbf{B}}{\partial t}, \tag{1.3c}$$

$$\nabla \times \mathbf{H} = \epsilon \frac{\partial \mathbf{E}}{\partial t} + \mathbf{J}_f + \frac{\partial \mathbf{P}}{\partial t}, \tag{1.3d}$$

https://doi.org/10.1017/S144618112300007X Published online by Cambridge University Press

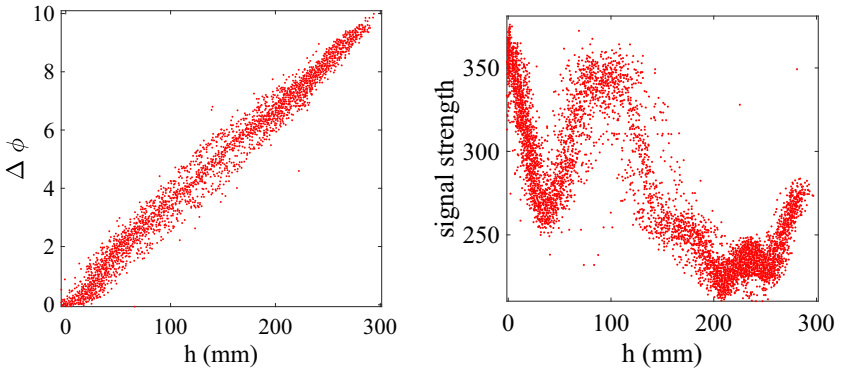


FIGURE 1. Microwave analyser data recorded while unloading bauxite from the ship Maia. The phase shift $\Delta\phi$ (radians) and signal strength ($-L$, the negative of attenuation; in arbitrary units for these data) are plotted against bauxite height.

where $\mathbf{E}$ is the electric field intensity, $\mathbf{P}$ is the polarization field of the dielectric, $\mathbf{H}$ the magnetic field intensity, $\mathbf{B} = \mu_0(\mathbf{H} + \mathbf{M}) = \mu\mathbf{H}$ is the magnetic induction, $\mathbf{J}_f$ is the free current density, $\mathbf{M}$ is the magnetization and $\rho_f$ the free charge density. The permittivity of free space (vacuum or air) is $\epsilon_0 = 8.85 \times 10^{-12}$ F/m and the permeability of free space is $\mu_0 = 4\pi \times 10^{-7}$ H/m which corresponds to the propagation speed (of light) $c = (\epsilon_0\mu_0)^{-1/2} \approx 3 \times 10^8$ m/s.

Boundary conditions at the interfaces between bauxite and air invoke continuity of normal and tangential electric and magnetic fields

$$[\epsilon\mathbf{E} \cdot \mathbf{n}]_-^+ = 0, \quad [\epsilon\mathbf{H} \cdot \mathbf{n}]_-^+ = 0, \quad [\mathbf{E} \times \mathbf{n}]_-^+ = 0, \quad [\mathbf{H} \times \mathbf{n}]_-^+ = 0,$$

where $\mathbf{n}$ is the unit normal to the interface, and the notation $[f]_-^+ = f^+ - f_-$ means the change in $f$ across the interface.

We treat the bauxite as a conducting dielectric porous medium, a material which is a mixture of solid, liquid and air. This mixture is considered to have an effective scalar conductivity $\sigma_b$ and an effective scalar permittivity $\epsilon_b$ that vary with moisture content, bauxite type and air content.

Polarization is taken to be in the same direction as $\mathbf{E}$ and proportional to it, so that $\mathbf{P} = \epsilon_0\chi_e\mathbf{E}$. The permittivity of the bauxite is written as $\epsilon_b = \epsilon_r\epsilon_0 = \epsilon_0(1 + \chi_e)$ and the permeability of the bauxite is $\mu_b = \mu_r\mu_0 = \mu_0(1 + \chi_m)$. Note that $\mathbf{J}_f = \sigma\mathbf{E}$.

Bauxite is usually considered to be nonmagnetic. However, it may contain maghemite, so that magnetization $\mathbf{M} = \chi_m\mathbf{H}$ may not be zero [7, 13, 17]. In soil science, a mass susceptibility or specific magnetic susceptibility is often calculated, which equals $\chi_m/\rho$, where $\rho$ is the bulk density of the soil. This mass susceptibility needs to be multiplied by bulk density (typically approximately 1200 kg/m$^3$ for mined bauxite) to obtain $\chi_m$.

Bauxites with high iron content [7] have measured values $\chi_m \approx 3 \times 10^{-4}$. Maghemite has mass susceptibility around $9 \times 10^{-4}$ m$^3$/kg [13], so that its bulk

https://doi.org/10.1017/S144618112300007X Published online by Cambridge University Press

magnetic susceptibility is $\chi_m \approx 1$. Weipa pisolith bauxite from Australia may contain up to 15% maghemite by mass [17] suggesting $\chi_m \approx 0.15n \approx 0.06$ for this bauxite if porosity $n = 0.4$.

Hence, $\mu_r = 1 + \chi_m$ is likely to be close to one for bauxite, and we will use $\mu_b = \mu_0$. Magnetization is also taken to be zero in the region representing the receiving antenna in the four-layer model, so that magnetic susceptibilities in air and in the antenna are set to $\mu = \mu_0$ in the following.

Our data are obtained at the operating frequency $f = 0.9$ GHz. At this frequency, water has $\epsilon_r \approx 80$ and $\sigma \approx 0.5$–$50$ mS/m depending on how potable it is. Seawater has $\epsilon_r \approx 80$ and $\sigma \approx 5000$ mS/m. Properties for damp soil provide some guidance as to anticipated values for bauxite. Measured permittivity results reviewed in [5] give for dryness near 0.02 (by volume, dry basis), $\epsilon_r \approx 3$ and $\sigma \approx 2$ mS/m for nearly dry silts, while for dryness near 0.4 (by volume, dry basis), $\epsilon_r \approx 24$ and $\sigma \approx 40$ mS/m for very wet silts.

**1.2. Differential equations** Taking the curl of (1.3c) and using

$$\nabla \times \nabla \times \mathbf{E} = -\nabla^2 \mathbf{E} + \nabla(\nabla \cdot \mathbf{E})$$

gives

$$\nabla^2 \mathbf{E} - \nabla(\nabla \cdot \mathbf{E}) = \frac{\partial}{\partial t}\left(\mu\epsilon \frac{\partial \mathbf{E}}{\partial t} + \mu \mathbf{J}_f + \mu \frac{\partial \mathbf{P}}{\partial t}\right),$$

and in the absence of free charges and using (1.3a), this becomes a wave equation for the electric field, which for constant material properties is [10, Section 27.8]

$$\nabla^2 \mathbf{E} - \mu\epsilon \frac{\partial^2 \mathbf{E}}{\partial t^2} - \mu\sigma \frac{\partial \mathbf{E}}{\partial t} = 0\ . \tag{1.4}$$

The same equation can be derived for the magnetic field strength $\mathbf{H}$, with $\mathbf{H}$ replacing $\mathbf{E}$.

**1.3. Simple model** A simple model that motivates the regression formula used in the microwave analyser considers transmission of microwaves that travel through a thickness $h$ of bauxite at a single frequency $\omega = 2\pi f$ before detection at the receiving antenna. Without loss of generality, we consider a polarized signal with fixed directions in which field strengths vary. Choosing origin at the base of the bauxite and axes aligned appropriately, we have solutions

$$\mathbf{H} = (0, H(x)e^{-i\omega t}, 0),$$
$$\mathbf{E} = (0, 0, E(x)e^{-i\omega t}),$$

where $i^2 = -1$. Equation (1.4) gives

$$\frac{\partial^2 E}{\partial x^2} = -\mu_b \omega^2 \epsilon_b E - i\mu_b \omega \sigma_b E. \tag{1.5}$$

https://doi.org/10.1017/S144618112300007X Published online by Cambridge University Press

The general solution is the complex-valued function of $x$

$$E = E_+ e^{ik_b x} + E_- e^{-ik_b x} \tag{1.6}$$

with arbitrary constants $E_\pm$. Substitution of this solution into (1.5) requires that the wavenumber $k_b$ in the bauxite satisfies the equation

$$k_b^2 = \omega^2 \epsilon_b \mu_b (1 + i\,\mathcal{D}_b).$$

The dissipation $\mathcal{D}_b = \sigma_b/(\omega\epsilon_b)$ is the magnitude of the conduction current density divided by the magnitude of the displacement current density [10] in bauxite.

The real part of $k_b$ may be written in the form [10, Section 11.3.1]

$$\mathrm{Re}(k_b) = \omega\sqrt{\frac{\epsilon_b\mu_b}{2}}\left(\sqrt{1+\mathcal{D}_b^2}+1\right)^{1/2},$$

while the imaginary part is

$$\mathrm{Im}(k_b) = \omega\sqrt{\frac{\epsilon_b\mu_b}{2}}\left(\sqrt{1+\mathcal{D}_b^2}-1\right)^{1/2}.$$

The choices of plus or minus in (1.6) correspond to waves travelling in the positive and negative $x$ directions when combined with the time dependence $e^{-i\omega t}$. The wave travelling upwards in the bauxite is attenuated as it moves away from origin, so that its amplitude reduces as $x$ increases above zero. The other wave grows in magnitude as $x$ increases. The usual assumption in this simple model is that $E_- = 0$ so that the electric field $E(x)$ does not grow without limit as $x$ increases. This is a modelling choice to consider the bauxite to be of infinite height, and to use $E(h)$ with $h$ the current measured height of the bauxite as a measure of the electric field at the receiving antenna. It is also a choice that does not allow any signal reflection at interfaces, for example, between bauxite and air.

Attenuation (reduction in electric wave amplitude with $h$) is then given in decibels by (1.2) for this simple model as

$$L_s = -20\log_{10}\left|\frac{E(h)}{E(0)}\right| = -20\log_{10} e^{-\mathrm{Im}(k_b)h} = 20\log_{10}(e)\,\mathrm{Im}(k_b)h.$$

For silts, dissipation $\mathcal{D} \approx 0.01$ so anticipating that dissipation is also much less than one for bauxite, it follows that $\mathrm{Im}(k_b) \approx \sqrt{\epsilon_b\mu_b}\,\mathcal{D}_b\omega/2$ and the attenuation is approximated for the simple model as

$$L_s \approx 10\log_{10}(e)\left(\sigma_b\sqrt{\frac{\mu_b}{\epsilon_b}}\right)h. \tag{1.7}$$

The coefficient of $h$ in (1.7) depends on moisture content through the effects of moisture on conductivity $\sigma_b$ and permittivity $\epsilon_b$. These effects may be nonlinear, but for small enough variations in moisture content, they will be approximately linear in moisture content. Furthermore, if moisture is almost constant, (1.7) says that attenuation is linear in $h$, which is wildly at odds with the data obtained for

https://doi.org/10.1017/S144618112300007X Published online by Cambridge University Press

attenuation or signal strength from the microwave analyser and plotted in Figure 1. This inconsistency between measured signal strength and linear model results raises an issue with the formula used by the microwave analyser to infer moisture content from attenuation.

The phase shift predicted by this simple model for small dissipation is

$$\Delta\theta = \arg\left(\frac{E(h)}{E(0)}\right) = \mathrm{Re}(k_b)h \approx \omega\sqrt{\epsilon_b\mu_b}\, h.$$

This prediction of a linear dependence of phase shift on bauxite height $h$, with slope varying with moisture content, is consistent with the appearance of phase shift versus $h$ seen from the data in Figure 1. It is also consistent with the formula used by the microwave analyser to predict moisture content.

These observations led the ESGI to recommend only using phase shift to infer moisture content. However, they left unresolved the question of why the attenuation data oscillate dramatically with $h$, beyond speculating that wave interference due to multiple internal reflections in the bauxite might be causing the issue.

**1.4. Reflections** Our aim is an improved model of the travelling electromagnetic waves in the microwave analyser between transmitting and receiving antenna, as they pass through intervening air and bauxite regions. We will use the differential equations (1.5) arising from Maxwell's equations to describe these waves.

The literature on travelling microwaves in granular material often leverages an equivalence to transmission line theory [4], and the branch relevant to the present application is referred to as free-space measurement of dielectric properties, in which plane microwaves are transmitted across an air gap to pass through a sample of known thickness and density before crossing another air gap to a receiving antenna [8, 14, 18].

Engineering electromagnetics texts such as that of Ulaby [20] show the equivalence of travelling electromagnetic waves in free space and in homogeneous media to the waves in transmission line theory, including the case of propagation through a slab [20, page 318]. However, the analysis is typically restricted to considerations like the critical thickness that makes a slab transparent.

There is good work on reflections within a single slab from the perspective of the shielding efficiency of planar materials [22]. In that paper, transmission through a slab of material of given thickness is modelled, with air above and below. Continuity conditions at the two interfaces are applied to solutions to correctly recover transmission and reflection terms. If we used their slab model, we would account for all reflections inside the bauxite. This would yield damped oscillations in signal strength versus $h$, with one wavelength that depended on bauxite properties. However, undamped reflections between bauxite and upper receiving antenna are also expected to occur within an air region which has a thickness that varies with bauxite height $h$. A model that combines the effects of reflection in bauxite and reflection in the overlying air gap may yield solutions that look more like our signal strength data in

https://doi.org/10.1017/S144618112300007X Published online by Cambridge University Press

Figure 1, which exhibits two or more different wavelengths when plotted against $h$. Hence, we develop a model that allows for reflections in both the bauxite and the overlying air gap.

In the remainder of this paper, we present a new four-layer model, air–bauxite–air–antenna, that captures the effects of multiple reflections within and above the bauxite. Using this model, we solve the four resulting coupled second-order differential equations for electric field strength and associated boundary or continuity conditions for all reflection and transmission coefficients, to find an expression for the electric signal at the receiving antenna. In this way, we capture the effects of an infinite number of reflections within the variable bauxite and air layers. We will also need to use ancillary models that relate bauxite mixture properties to moisture content. Our solution provides improved matches to our signal strength data, increases our understanding of the analyser behaviour and leads to recommendations for improved moisture measurements of conveyor materials using microwave technology.

## 2. Four-layer model

We now develop a four-layer model, in which microwaves transmitted by the lower antenna travel through an air gap below the bauxite layer, then through a bauxite layer of variable height $h$, to cross another air gap before detection by a receiving antenna. The geometry is illustrated with the four numbered regions in order of increasing $x$, air, bauxite, air and conductor, in Figure 2, with microwaves assumed to travel in the $x$-direction normal to planar air/bauxite and air/antenna interfaces. Changes in bauxite height occur on a time scale of seconds, much slower than the speed of the microwaves.

We assume the fields incident upon the base of the bauxite are free space plane waves. The transmitting antenna emits a combination of electric and magnetic fields that vary with distance in the near-field in a complicated fashion, which decrease with an inverse dependence on distance that changes from cubic to quadratic to linear, at distances much less than $\lambda/(2\pi)$ from the antenna, where $\lambda$ is the wavelength of the microwave radiation in air. The electromagnetic fields are close to free space propagation fields with constant amplitudes in the far-field at distances greater than $\lambda/(2\pi)$ [10]. For the frequency $f$ =900 MHz used in the analyser, the wavelength is approximately 333 mm, using $\lambda = c/f$, where the speed of light is $c \approx 3 \times 10^8$ m/s.

Then a far-field assumption is plausible when the bauxite begins at distances at or greater than approximately 55 mm from the transmitting antenna. This requirement is taken to be met by the analyser setup, as the distances from antenna wires to the base of the conveyor belt are at least 45 mm, and in practice appear to be close to 100 mm.

Then, in region 1, we have plane wave solutions

$$\mathbf{H}_1 = (0, H_1(x)e^{-i\omega t}, 0),$$
$$\mathbf{E}_1 = (0, 0, E_1(x)e^{-i\omega t}),$$

https://doi.org/10.1017/S144618112300007X Published online by Cambridge University Press

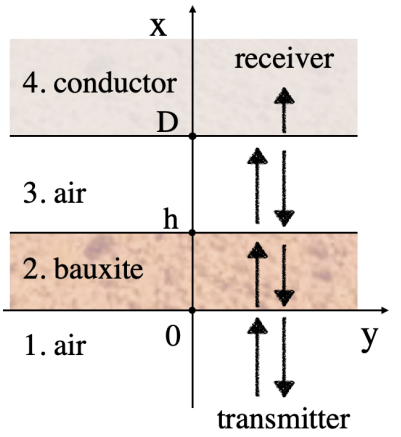


FIGURE 2. Sketch of four-layer model, showing regions 1–4. The bauxite layer extends from $x = 0$ to the variable height $x = h$, and the air layer between bauxite and upper antenna extends from $x = h$ to a fixed location $x = D$.

where $E_1(x)$ satisfies the differential equation

$$\frac{\partial^2 E_1}{\partial x^2} = -\mu_0 \omega^2 \epsilon_0 E_1, \tag{2.1}$$

and $H_1$ satisfies the same equation as $E_1$. Fundamental solutions take the form

$$e^{\pm ikx},$$

and substitution into (2.1) gives

$$k^2 = \omega^2 \epsilon_0 \mu_0 = \frac{\omega^2}{c^2},$$

where $k$ is the wavenumber in free space or air, for which $k = 2\pi/\lambda$ and $\lambda$ is the wavelength in free space. Without loss of generality, we choose $k = \omega/c = \omega\sqrt{\epsilon_0 \mu_0}$. The impedance $Z_0 = \mu_0 \omega/k = k/(\omega\epsilon_0) = \sqrt{\mu_0/\epsilon_0} \approx 377$ ohms will be a useful combination of parameter values.

The general solution is a linear combination of the two fundamental solutions. One ($e^{ikx}$) corresponds to a wave travelling in the positive $x$-direction, and is called the incident wave. The other is a reflected wave travelling in the negative $x$-direction in region 1.

The wave in the air in region 1 where $x \leqslant 0$ that is incident upon the bauxite is given by

$$\begin{aligned} \mathbf{H}_i &= (0, e^{ikx - i\omega t}, 0), \\ \mathbf{E}_i &= (0, 0, -Z_0 e^{ikx - i\omega t}). \end{aligned} \tag{2.2}$$

Without loss of generality, we take the amplitude of the incident magnetic field $\mathbf{H}_i$ to be one in value. Other terms are in essence normalized by it. The amplitude of the

https://doi.org/10.1017/S144618112300007X Published online by Cambridge University Press

electric field in (2.2) follows from Maxwell's equation (1.3d). In region 1, there are no polarisers and the free current density is zero, so (1.3d) may be written in the form $\nabla \times \mathbf{H} = -i\omega\epsilon_0\mathbf{E}$, and this leads to the $Z_0$ term in (2.2). In region 1, the reflected wave is of unknown amplitude $R$, and is given by

$$\mathbf{H}_r = (0, Re^{-ikx-i\omega t}, 0),$$
$$\mathbf{E}_r = (0, 0, RZ_0e^{-ikx-i\omega t}).$$

In region 2, where $0 \leqslant x \leqslant h$, the waves are travelling through the bauxite mixture with fields described as in Section 1.3 by

$$\mathbf{H} = (0, H(x), 0)e^{-i\omega t}, \quad \mathbf{E} = (0, 0, E(x))e^{-i\omega t},$$

with solutions for $E(x)$

$$E = E_+e^{ik_bx} + E_-e^{-ik_bx}. \tag{2.3}$$

The amplitudes $E_+$ and $E_-$ of the upwards and downwards travelling waves will be determined by applying boundary conditions. Note that this approach allows for reflections at air/bauxite interfaces, in contrast to the approach taken in Section 1.3.

In the air in region 3, where $h \leqslant x \leqslant D$, there is a transmitted wave travelling upwards of unknown amplitude $T$ given by

$$\mathbf{H}_t = (0, Te^{ikx-i\omega t}, 0),$$
$$\mathbf{E}_t = \left(0, 0, -\left(\frac{kT}{\epsilon_0\omega}\right)e^{ikx-i\omega t}\right),$$

and a reflected wave coming back from the receiving antenna, of unknown amplitude $R_2$:

$$\mathbf{H}_{r2} = (0, R_2e^{-ikx-i\omega t}, 0),$$
$$\mathbf{E}_{r2} = \left(0, 0, \left(\frac{kR_2}{\epsilon_0\omega}\right)e^{-ikx-i\omega t}\right).$$

In region 4, the receiving antenna will be modelled as a semi-infinite material with relatively high electrical conductivity, with the analyser signal that provides our data assumed to be drawn from an antenna that is at the surface of that material at $x = D$. In the antenna region $x \geqslant D$, we have the fields

$$\mathbf{H}_a = (0, H_a(x), 0)e^{-i\omega t},$$
$$\mathbf{E}_a = (0, 0, E_a(x))e^{-i\omega t}.$$

In the antenna, (1.5) applies but with the effective properties of the antenna material indicated by subscripts $a$, so that

$$\frac{\partial^2 E_a}{\partial x^2} = -\mu\omega\sigma_a\left[\left(\frac{\omega\epsilon_a}{\sigma_a}\right)E_a + iE_a\right]. \tag{2.4}$$

https://doi.org/10.1017/S144618112300007X Published online by Cambridge University Press

The general solution to (2.4) can be written as

$$E_a = A_+ e^{ik_a(x-D)} + A_- e^{-ik_a(x-D)}.$$

Substitution of this solution into (2.4) requires that the wavenumber $k_a$ in the antenna satisfies the equation

$$k_a^2 = \omega^2 \epsilon_a \mu \left(1 + i\frac{\sigma_a}{\omega \epsilon_a}\right),$$

and the constants $A_\pm$ are to be determined. The electromagnetic properties of the receiving antenna are not known to us. They could be chosen to be those of an almost lossless 50 ohm transmission line. Choosing the root $k_a$ without loss of generality to be the one with positive imaginary part, vanishing of $E_a$ as $x \to \infty$ requires that $A_- = 0$.

There are three unknown transmission and reflection coefficients $R$, $T$ and $R_2$, plus two unknown amplitudes $E_+$ and $E_-$ in the bauxite, and the remaining unknown coefficient $A_+$ in the receiving antenna. These six unknown constants are provided by three pairs of boundary conditions which give six linear equations that are to be solved simultaneously.

The pair at $x = 0$ is given as follows. Continuity of the tangential component of $\mathbf{H}$ gives $H(0) = 1 + R$. In the bauxite, Maxwell's equation (1.3c) gives

$$\nabla \times \mathbf{E} = -\mu_b \frac{\partial \mathbf{H}}{\partial t},$$

so that

$$\frac{\partial E}{\partial x} = -i\omega\mu_b H, \tag{2.5}$$

and then

$$\frac{\partial E}{\partial x} = -i\mu_b \omega (1 + R). \tag{2.6}$$

Continuity of the tangential component of $\mathbf{E}$ directly gives

$$\frac{k}{\epsilon_0 \omega}(R - 1) = E(0). \tag{2.7}$$

The pair at $x = h$ is given in a similar manner. Continuity of $\mathbf{H} \times \mathbf{n}$ gives $H(h) = Te^{ikh} + R_2 e^{-ikh}$, so that (2.5) yields

$$\frac{\partial E}{\partial x} = -i\mu_b \omega (Te^{ikh} + R_2 e^{-ikh}), \tag{2.8}$$

and continuity of $\mathbf{E} \times \mathbf{n}$ yields

$$E(h) = -\left(\frac{k}{\epsilon_0 \omega}\right)(Te^{ikh} - R_2 e^{-ikh}). \tag{2.9}$$

https://doi.org/10.1017/S144618112300007X Published online by Cambridge University Press

At the antenna $x = D$, continuity of $\mathbf{H} \times \mathbf{n}$ gives $H_a = Te^{ikD} + R_2 e^{-ikD}$, so that (2.5) (but using antenna properties) gives

$$\frac{\partial E_a}{\partial x} = -i\mu_0\omega(Te^{ikD} + R_2 e^{-ikD}), \tag{2.10}$$

and continuity of $\mathbf{E} \times \mathbf{n}$ gives

$$E_a(D) = -\left(\frac{k}{\epsilon_0\omega}\right)(Te^{ikD} - R_2 e^{-ikD}). \tag{2.11}$$

It is helpful to set up the boundary conditions as a matrix problem to be solved for the six unknowns $E_+$, $E_-$, $R$, $T$, $R_2$ and $A_+$. We are particularly interested in finding $A_+$, giving us the signal in the receiving antenna. Equations (2.6) and (2.7) give

$$E_+ + E_- - Z_0 R = -Z_0, \tag{2.12}$$

$$E_+ - E_- + Z_b R = -Z_b, \tag{2.13}$$

where $Z_b = \mu_b\omega/k_b$ is the impedance of the bauxite mixture. Equations (2.8) and (2.9) together with (2.3) give

$$e^{ik_b h}E_+ - e^{-ik_b h}E_- + Z_b e^{ikh}T + Z_b e^{-ikh}R_2 = 0,$$
$$e^{ik_b h}E_+ + e^{-ik_b h}E_- + Z_0 e^{ikh}T - Z_0 e^{-ikh}R_2 = 0.$$

Equations (2.10) and (2.11) together with $E_a = A_+ e^{ik_a(x-D)}$ give

$$Z_a e^{ikD}T + Z_a e^{-ikD}R_2 + A_+ = 0, \tag{2.14}$$

$$Z_0 e^{ikD}T - Z_0 e^{-ikD}R_2 + A_+ = 0, \tag{2.15}$$

where $Z_a = \mu_0\omega/k_a$ is the impedance of the region representing the receiving antenna. Then (2.12)–(2.15) can be written in matrix form:

$$\begin{pmatrix} 1, & 1, & -Z_0, & 0, & 0, & 0 \\ 1, & -1, & Z_b, & 0, & 0, & 0 \\ e^{ik_b h}, & -e^{-ik_b h}, & 0, & Z_b e^{ikh}, & Z_b e^{-ikh}, & 0 \\ e^{ik_b h}, & e^{-ik_b h}, & 0, & Z_0 e^{ikh}, & -Z_0 e^{-ikh}, & 0 \\ 0, & 0, & 0, & Z_a e^{ikD}, & Z_a e^{-ikD}, & 1 \\ 0, & 0, & 0, & Z_0 e^{ikD}, & -Z_0 e^{-ikD}, & 1 \end{pmatrix} \begin{pmatrix} E_+ \\ E_- \\ R \\ T \\ R_2 \\ A_+ \end{pmatrix} = \begin{pmatrix} -Z_0 \\ -Z_b \\ 0 \\ 0 \\ 0 \\ 0 \end{pmatrix},$$

and represented as the augmented matrix

$$\left(\begin{array}{cccccc|c} 1, & 1, & -Z_0, & 0, & 0, & 0 & -Z_0 \\ 1, & -1, & Z_b, & 0, & 0, & 0 & -Z_b \\ e^{ik_b h}, & -e^{-ik_b h}, & 0, & Z_b e^{ikh}, & Z_b e^{-ikh}, & 0 & 0 \\ e^{ik_b h}, & e^{-ik_b h}, & 0, & Z_0 e^{ikh}, & -Z_0 e^{-ikh}, & 0 & 0 \\ 0, & 0, & 0, & Z_a e^{ikD}, & Z_a e^{-ikD}, & 1 & 0 \\ 0, & 0, & 0, & Z_0 e^{ikD}, & -Z_0 e^{-ikD}, & 1 & 0 \end{array}\right).$$

https://doi.org/10.1017/S144618112300007X Published online by Cambridge University Press

Gauss–Jordan row reduction gives an upper triangular augmented matrix which allows to read off the solutions

$$\left(\begin{array}{cccccc|c} 1, & 0, & (Z_b - Z_0)/2, & 0, & 0, & 0 & -(Z_0 + Z_b)/2 \\ 0, & 1, & -(Z_b + Z_0)/2, & 0, & 0, & 0 & (Z_b - Z_0)/2 \\ 0, & 0, & (Z_b + Z_0)e^{-ik_b h}, & (Z_0 - Z_b)e^{ikh}, & -(Z_0 + Z_b)e^{-ikh}, & 0 & (Z_0 - Z_b)e^{-ik_b h} \\ 0, & 0, & 0, & Ae^{ikh}, & Be^{-ikh}, & 0 & C \\ 0, & 0, & 0, & 0, & 2Z_0 Z_a e^{-ikD}, & Z_0 - Z_a & 0 \\ 0, & 0, & 0, & 0, & 0, & F & -2CZ_0 Z_a \end{array}\right),$$

where

$$\begin{aligned} A &= (Z_0 - Z_b)^2 e^{ik_b h} - (Z_0 + Z_b)^2 e^{-ik_b h}, \\ B &= (Z_b^2 - Z_0^2)(e^{ik_b h} - e^{-ik_b h}), \\ C &= (Z_0 - Z_b)^2 - (Z_0 + Z_b)^2 = -4Z_0 Z_b \end{aligned}$$

and

$$F = B(Z_0 - Z_a)e^{ik(D-h)} + A(Z_0 + Z_a)e^{-ik(D-h)}.$$

It follows that the signal at the surface of the receiving antenna is

$$A_+ = -\frac{2CZ_0 Z_a}{F}. \tag{2.16}$$

Note that $F$ depends on $k(D - h)$, and through $A$ and $B$, it depends also on $k_b h$, giving two different wavelengths versus $h$, one determined by free-space properties in the real part of $k$ and the other by bauxite properties in the real part of $k_b$.

The other unknowns can now be computed by back-substitution, for example, row 5 now gives

$$2Z_0 Z_a e^{-ikD} R_2 + (Z_0 - Z_a)A_+ = 0,$$

so that

$$R_2 = \frac{C}{F}(Z_0 - Z_a)e^{ikD}.$$

A simple way to obtain (2.16) for $A_+$ (and all of the other unknowns) is to use MATLAB's command

```
syms Z0 Za Zb k kb h D
```

to set up symbols for each term in the matrix, then use the `rref` command on the augmented symbolic matrix to return the reduced row echelon form using Gauss–Jordan elimination with partial pivoting. The returned solution components are in symbolic form, and are expanded-out versions of what is obtained by hand above. They provided us with a useful check against errors in our hand calculations.

https://doi.org/10.1017/S144618112300007X Published online by Cambridge University Press

Other forms for $A_+$ are

$$A_+ = \frac{8Z_0^2 Z_a Z_b \; e^{ikD} e^{ikh} e^{ik_b h}}{F_2},$$

where

$$F_2 = (Z_b^2 - Z_0^2)(Z_0 - Z_a)(e^{2ik_b h} - 1)e^{2ikD} + [(Z_0 - Z_b)^2 e^{2ik_b h} - (Z_0 + Z_b)^2](Z_0 + Z_a)e^{2ikh}, \tag{2.17}$$

and

$$A_+ = \frac{2(1 - R_\infty)Z_0 Z_a}{(Z_0 + Z_a)F_3},$$

where

$$F_3 = R_a R_\infty (e^{-ik_b h} - e^{ik_b h})e^{ik(D-h)} + (R_\infty^2 e^{ik_b h} - e^{-ik_b h})e^{-ik(D-h)}$$

and

$$R_\infty = \frac{Z_0 - Z_b}{Z_0 + Z_b}, \quad R_a = \frac{Z_0 - Z_a}{Z_0 + Z_a}. \tag{2.18}$$

The term labelled $R_\infty$ is the reflection coefficient that would apply at $x = 0$ if the bauxite height $h \to \infty$. This standard result can be seen in our four-layer model if we set $E_-$ to zero (so that there is no reflection from $x = h$, or that $|E| \to 0$ in the bauxite as $h \to \infty$), so that (2.12) and (2.13) become, after replacing $R$ with $R_\infty$,

$$E_+ - Z_0 R_\infty = -Z_0, \quad E_+ + Z_b R_\infty = -Z_b.$$

Now $E_+$ can be eliminated to give the form (2.18) for $R_\infty$.

As the bauxite height $h \to 0$, it follows that $A \to C$ and $B \to 0$ and $F \to C(Z_0 + Z_a)e^{-ikD}$. Then in the absence of bauxite, the magnitude of the received signal becomes, using (2.16),

$$|A_+| \to \left|\frac{2Z_0 Z_a}{Z_0 + Z_a}\right|, \quad h \to 0. \tag{2.19}$$

We see in (2.19) that, in general, the magnitude $|A_+|$ of the received signal does not simplify to the magnitude of the transmitted electric field ($Z_0$) as $h \to 0$. This is due to the mismatch between the free-space impedance $Z_0$ used for the transmitted wave in region 1, and the impedance $Z_a$ of the receiving antenna. The detected power tends to the transmitted power (and attenuation tends to zero, or $|Z_0/A_+|$ tends to one) as $h \to 0$ only in the unrealistic case that the impedance $Z_a$ of the receiving antenna is matched to $Z_0$.

The impact of bauxite and its attendant moisture on the analyser setup is naturally measured by using, say (2.16), to provide the zero bauxite value for the response of the receiving antenna as the reference signal,

https://doi.org/10.1017/S144618112300007X Published online by Cambridge University Press

$$A_+^0 = \lim_{h\to 0} A_+ = -\left(\frac{2Z_0 Z_a}{Z_0 + Z_a}\right) e^{ikD},$$

which captures the instrumental effect of mismatched impedances between transmitting and receiving antennae. Then using (2.16) again, the dependence of $A_+$ on $h$ relative to the zero bauxite value $A_+^0$ is given by

$$A_{4\mathrm{L}}^0 = 20\log_{10}\left|\frac{A_+^0}{A_+}\right| = 20\log_{10}\left|\frac{F}{C(Z_0 + Z_a)}\right|.$$

This provides the decibel measure of attenuation due to the presence of bauxite mixture on the belt, and is zero in the limit $h \to 0$.

The attenuation then depends on bauxite thickness $h$ via exponents involving $ikh$ and $ik_b h$, that is, combinations of sinusoids with magnitudes that have wavelengths $\pi/k \approx 166$ mm and $\pi/\mathrm{Re}(k_b) \approx 30$–$80$ mm (using damp silt properties).

The terms appearing in (2.17), which forms part of the detected electric field $A_+$, involve $e^{2ik_b h}$ and $e^{2ikh}$, indicating that reflections cause the observed oscillations to have half the wavelengths of travelling waves without reflections present.

That is, our four-layer model predicts wavelengths of 83 mm and 15–40 mm, consistent with what is seen in the graph of signal strength data versus $h$ in Figure 1. The longer wavelength is associated with reflections occurring in region 3 above the bauxite, while the shorter is associated with reflections occurring inside the bauxite in region 2.

A simple physical explanation that ignores attenuation for reflections within the bauxite slab causing constructive interference effects with wavelengths that are half of those of the travelling wave can be made. The first and largest reflected wave travels a distance $3h$ compared with a nonreflected wave travelling a distance $h$. Adding sinusoids $\sin(kh) + \sin(3kh)$ gives a term depending on $2kh$ from the sin sum formula, that is, half the wavelength of a $kh$ term.

The signal strength data from the analyser are to be compared with our four-layer model prediction,

$$SS = -A_{4\mathrm{L}}^0 = -20\log_{10}\left|\frac{A_+^0}{A_+}\right| = 20\log_{10}\left|\frac{A_+}{A_+^0}\right|,$$

and the phase shift data derived from analyser output [12] are to be compared with our model

$$\Delta\phi = \mathtt{angle}\left(\frac{A_+}{A_+^0}\right).$$

Important parameters are the distance $D$ between the upper antenna and the unloaded conveyor belt, the permittivity $\epsilon_r$ and the electric conductivity $\sigma_b$ of the bauxite mixture. We now compare the behaviour of our four-layer model to the data from the microwave analyser.

https://doi.org/10.1017/S144618112300007X Published online by Cambridge University Press

## 3. Results

We examine the effects of three important parameters $D$, $\epsilon_r$ and $\sigma$ on the solution to our model, while comparing with data.

**3.1. Distance $D$** The ranges of $D$ values investigated were chosen after studying technical drawings of the microwave analyser, which give the distance between the inner surfaces of the antenna housings as approximately 600 mm. The housings are each 120 mm thick. The drawings do not reveal the exact structure of the antennae, or where inside the housings the wires are, so there is some uncertainty in the correct value for $D$. We have compared model results to data to help determine an accurate value for $D$, and we found they are sensitive to changes in $D$ of just a few millimetres.

We noticed that for a signal strength, smaller $D$ values matched data from smaller bauxite heights, while larger $D$ values did better at larger heights, suggesting conveyor belt sag might be affecting the data. Conveyor belt sag affects measured bauxite height since the ultrasound sensor is mounted above the bauxite looking down on it, so any sag means the true bauxite height is larger than measured. Sag also increases the distance $D$ from the bottom of the bauxite to the receiving antenna, making it a function of $h$. We found improved matches to signal strength data when we adjusted original data heights $h_0$ to a true height $h$ using

$$h = h_0 + \mathtt{sag},$$

and we used in our model

$$D = D_0 + \mathtt{sag},$$

where $D_0$ is the distance from empty belt to receiving antenna, and where

$$\mathtt{sag} = \frac{S_m}{\pi}(\arctan((h - h_0)/S_e) + \arctan(h_0/S_e))$$

with maximum sag $S_m = 0.1$ m, centre of sag $h_0 = 0.25$ m and extent $S_e = 0.05$ m. The resulting sag values and adjusted height values are illustrated in Figure 3.

We compute signal strength and phase shift for a range of values for the distance $D_0$ and, as illustrated in Figure 4, the model signal strength is very sensitive to this distance, as it strongly affects the interference effect in region 3 between bauxite and receiving antenna. Changes of just 5 mm in $D_0$ have a significant effect on signal strength when plotted against $h$. Good matches to signal strength are seen with 70 mm maximum belt sag but the phase shift data do not give a good match to the model when this much belt sag is used. We also see that phase shift is much less sensitive to changes in $D_0$.

Reducing the belt sag to have a maximum of 40 mm (and reducing $\epsilon_r$ to a value of 6.2) leads to a better overall match, as illustrated in Figure 5, but at the expense of the signal strength match. The alignment of phase shifts at higher $h$ values indicates that belt sag is better set to zero. The data acquired at smaller $h$ values are relatively noisy, and are subject to timing issues as the bauxite height typically only passes briefly

https://doi.org/10.1017/S144618112300007X Published online by Cambridge University Press

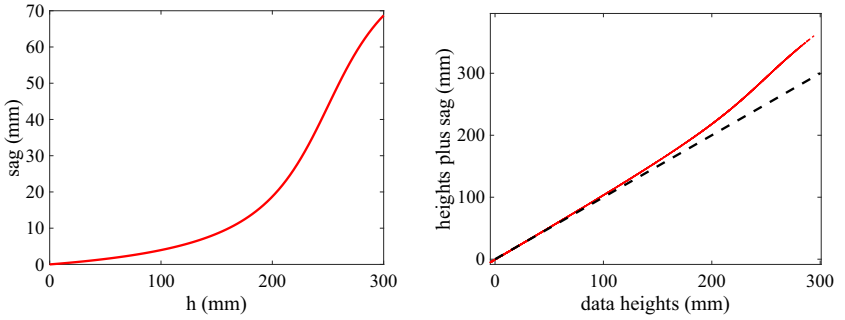


FIGURE 3. Conveyor belt sag used to improve matches between data and our four-layer model. The effect of the sag on measured bauxite heights is illustrated in the right-hand plot. The dashed line indicates zero sag values and the solid line shows height values corrected for sag.

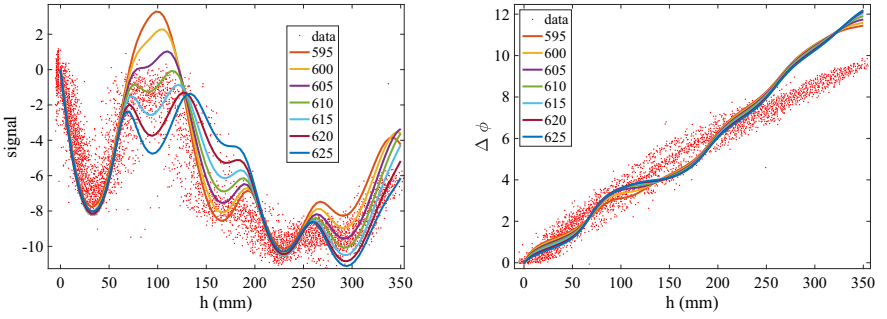


FIGURE 4. Comparisons of our four-layer model results with microwave analyser data, for varying values of the distance $D_0$ (mm) between empty belt and receiving antenna. The $D_0$ values generating model results (lines) are listed in the legend and data are represented by dots. Antenna properties are taken to be $\epsilon_a = \epsilon_0$ and $\sigma_a = 50$ S/m, and bauxite properties are $\epsilon_r = 6.5$ and $\sigma_b = 30$ mS/m. Belt sag maximum is 70 mm.

through these value, with approximately six values recorded each time the belt goes between unloaded and the typical full load of 200–250 mm height. So we set zero sag for the remaining model simulations in this paper, and we will use $D_0 = 0.615$.

**3.2. Inferring permittivity and conductivity** We now explore implications of the four-layer model for inferring the permittivity and the electrical conductivity of the bauxite mixture from the signal strengths, phase shifts and bauxite heights provided by the microwave analyser.

Four-layer model responses are illustrated for varying bauxite relative permittivities in Figures 6 and 7, with fixed $D = 0.615$ m. The signal strength curves cross each other in multiple locations, in contrast to the phase shifts which look much more useful for inferring bauxite permittivity.

https://doi.org/10.1017/S144618112300007X Published online by Cambridge University Press

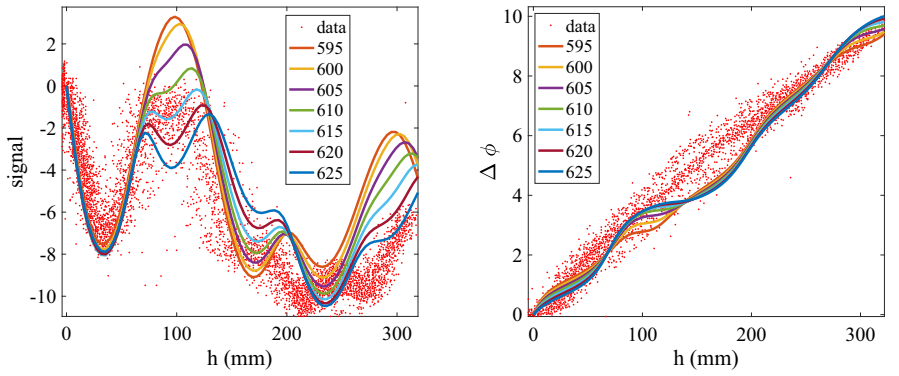


FIGURE 5. Comparisons of our four-layer model results with microwave analyser data for varying values of the distance $D_0$ (mm) between empty belt and receiving antenna. The $D_0$ values generating model results (lines) are listed in the legend and data are represented by dots. Antenna properties are taken to be $\epsilon_a = \epsilon_0$ and $\sigma_a = 50$ S/m, and bauxite properties are $\epsilon_r = 6.2$ and $\sigma_b = 30$ mS/m. Belt sag maximum is 40 mm.

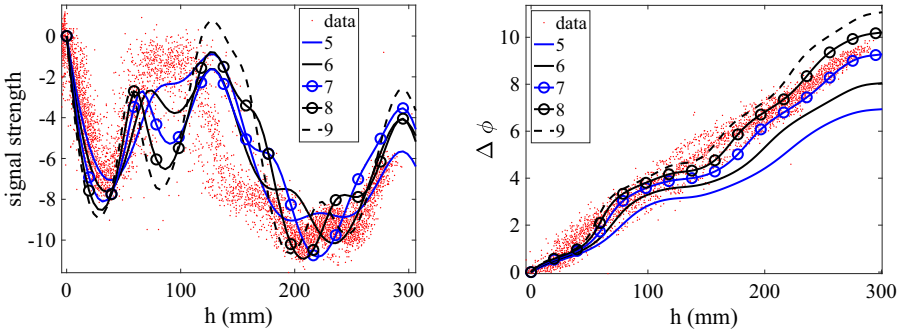


FIGURE 6. Comparisons of our four-layer model results with microwave analyser data for varying values of the bauxite mixture permittivity. The $\epsilon_r$ values generating model results (lines) are listed in the legend and data are represented by dots. Antenna properties are taken to be $\epsilon_a = \epsilon_0$ and $\sigma_a = 50$ S/m, and bauxite conductivity is fixed at $\sigma_b = 35$ mS/m. The distance $D = 0.615$ m is fixed. Belt sag is zero. Signal strengths are in dB. Phase shifts are in radians.

The crossings of the curves of constant permittivity in the signal strength plots are indicative of noninvertible graphs of permittivity versus signal strength at given $h$ values. That is, folds in the surface indicate where there is more than one permittivity value giving a particular value of signal strength (given $h$), so that the signal data cannot in general be used to infer permittivity.

This may be clearer in the visualization of the signal strength as a function of $h$ and $\epsilon_r$ shown in the waterfall plot in Figure 8. Here are plotted curves of constant $h$, which reveal that sometimes a single data value for signal strength $SS$ may be obtained by more than one choice of $\epsilon_r$. This becomes clear when considering $SS$–$\epsilon_r$ planes at

https://doi.org/10.1017/S144618112300007X Published online by Cambridge University Press

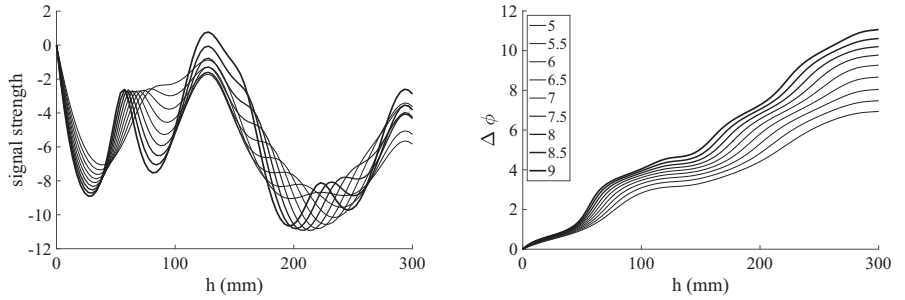


FIGURE 7. Four-layer model results with varying values of the bauxite mixture permittivity. A simpler line style and more finely spaced permittivity values are used to make clearer the appearance of the surface, that is, $\epsilon_r$ as a function of signal strength and $h$, through its level curves. Other parameter values are the same as in Figure 6.

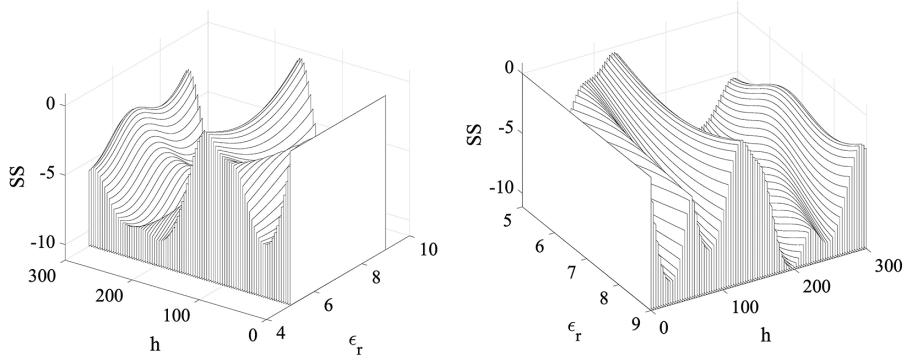


FIGURE 8. Four-layer model signal strength (*SS*, in dB) results visualized as waterfall plots using two different view points. They show *SS* as a surface, a function of $h$(mm) and bauxite mixture permittivity $\epsilon_r$. Antenna properties are taken to be $\epsilon_a = \epsilon_0$ and $\sigma_a = 50$ S/m, and bauxite conductivity is fixed at $\sigma_b = 35$ mS/m.

a given $h$ value, featuring curves that fail the horizontal line test for invertibility. For example, there are two choices for $\epsilon_r$ near $h = 150$ giving $SS = -2$, or three choices for $\epsilon_r$ near $h = 250$ giving $SS = -7$. However, model phase shifts are invertible, and do provide a single value of permittivity – at any given $h$, a value for phase shift is clearly associated with just one bauxite permittivity value.

The four-layer model responses as the bauxite mixture electric conductivity is varied are illustrated in Figure 9, with fixed $D = 0.615$ m. The signal strength curves now look much more useful for inferring bauxite conductivity, if permittivity is constant. The phase shifts however are very insensitive to conductivity, and on close inspection, they also cross over each other as $h$ varies.

Recalling that measurements on silts [5] have both relative permittivity and conductivity of the mixture increasing with moisture content, it remains unclear whether

https://doi.org/10.1017/S144618112300007X Published online by Cambridge University Press

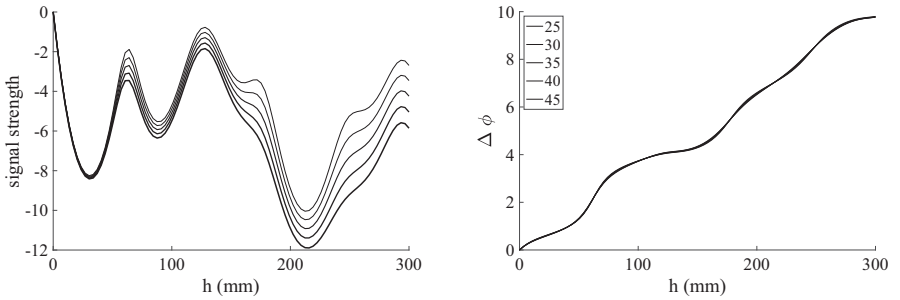


FIGURE 9. Four-layer model results with varying values of the bauxite mixture conductivity. The $\sigma_b$ values generating model results (lines) are listed in the legend with units mS/m. Antenna properties are taken to be $\epsilon_a = \epsilon_0$ and $\sigma_a = 50$ S/m, and bauxite relative permittivity is fixed at $\epsilon_r = 7.5$.

either signal strength or phase shift can be used to infer moisture content without further analysis of the relationships between moisture content and electromagnetic mixture properties. The broad implications of the modelling here are that the effects of reflections could be very unhelpful for inferring moisture content.

Changing the spacing of the antenna does not improve things at current microwave analyser settings – variations of bauxite height as the conveyor goes between empty and full are of the same order as the wavelength of the microwaves in air. Deciding to only use measurements taken near a fully loaded conveyor belt does not help, as changes in bauxite moisture at any given value of $h$ are always dominated by reflection, overwhelming the inference of electromagnetic properties and thence moisture content.

## 4. Frequency reduction

Reducing the microwave operating frequency is one possible approach to improving the usefulness of the analyser, with encouraging results from our model as illustrated in Figures 10 and 11, where frequency is one-tenth of the usual analyser operating frequency. The longer wavelength of more than 3 m now means there is less interference from reflected waves over the relatively smaller distances $h$ and $D - h$.

Then signal strength variations are nicely correlated to changes in electrical conductivity, and would be expected to provide accurate predictions of conductivity using linear correlations. However, phase shifts have relatively small changes when conductivity is varied, and are not invertible for some values of $h$.

However, signal strength varies little with permittivity and is not invertible, while phase shifts have a very regular dependence on permittivity, implying that they can be calibrated with a linear approach to accurately predict the permittivity of a bauxite mixture. The usefulness of this approach remains to be seen for inferring moisture content, but it has been to some degree successful in reducing reflection effects on some of the data.

https://doi.org/10.1017/S144618112300007X Published online by Cambridge University Press

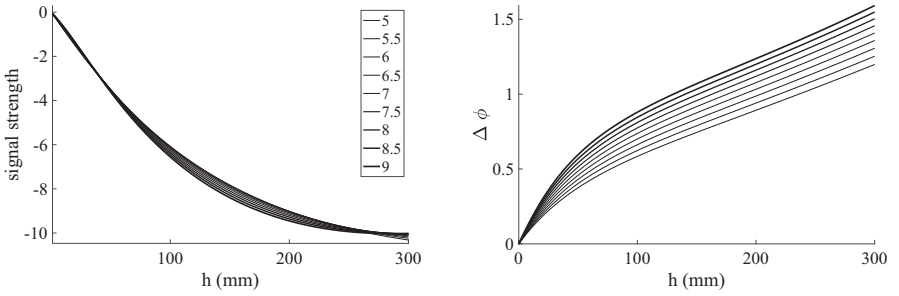


FIGURE 10. Four-layer model results with frequency lowered to 0.09 GHz. The $\epsilon_r$ values generating signal strengths and phase shifts (lines) are listed in the legend. Antenna properties are taken to be $\epsilon_a = \epsilon_0$ and $\sigma_a = 50$ S/m, and bauxite electrical conductivity is fixed at $\sigma = 35$ mS/m. Sag is zero.

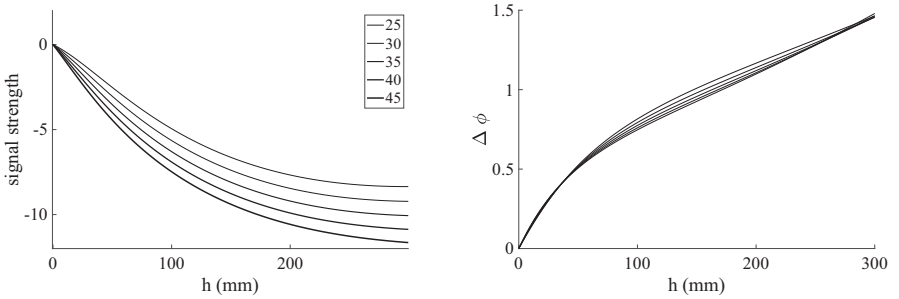


FIGURE 11. Four-layer model results with frequency lowered to 0.09 GHz. The $\sigma$ values generating model results (lines) are listed in the legend. Antenna properties are taken to be $\epsilon_a = \epsilon_0$ and $\sigma_a = 50$ S/m, and bauxite relative permittivity is fixed at $\epsilon_r = 7.5$. Sag is zero.

## 5. Conclusions

Time-domain gating techniques [4, 9, 19] derive from reflectometry techniques for detecting discontinuities in a conducting or dielectric medium, and can be designed to avoid the effects of multiple internal reflections. They have been used since the 1960's, and are standard in some network analysers. They are known to improve results when detecting grain moisture content using free space microwave measurements [9]. These gating techniques allow the extraction of the very first travelling wave received when the lower antenna begins transmission. Then reflections do not have time to affect the received signal, and we expect that a linear calibration approach, as outlined at the beginning of this paper, will be more effective in combination with gating. Our four-layer model results will not apply, since the boundary conditions at $x = h$ and $x = D$ will not have time to take effect.

However, the time taken between a pulse first reaching the upper antenna and the first reflection from that antenna then reflecting off the top of the bauxite and back through the air in region 3 is approximately 2 ns, which is the only time for two oscillations at the transmitted frequency of 0.1 GHz. So time-domain gating techniques

https://doi.org/10.1017/S144618112300007X Published online by Cambridge University Press

might have difficulty removing the first reflection in region 3, and will require the transmitter to initiate the signal in less than a nanosecond.

Bauxite surface roughness and slope can lead to significant errors in our modelling and present challenging prospects for improving our approach. Dobson and Ulaby [5] recommended using variable frequencies in the context of active microwave radiation to detect the moisture content of soils by remote sensing.

We have assumed a well-mixed effective medium for the mixture of bauxite, water and air on the conveyor belt. Our four-layer model accounts for attenuation within the bauxite layer, and for interference due to reflections at air/bauxite and air/antenna interfaces. We have not considered the possibility of internal reflections within the bauxite layer arising from possible variations in moisture content with depth, giving additional internal layering effects. Interesting questions remain including the possibility of using an effective bauxite height that may be different from that measured by the ultrasound device and that may allow better matches to signal strength data.

Our four-layer model has successfully reproduced many of the signal strength details that puzzled participants in the 2017 Study Group, and is a big improvement on the semi-infinite linear model. Despite not matching every detail of signal strength and phase shift seen in the data, the four-layer model provides useful insight into microwave analyser behaviour. An important insight is that interference due to reflections in the region between bauxite and receiving antenna is responsible for the large oscillations seen in signal strength when plotted against bauxite height. These are superposed upon, and dominate, the expected shorter wavelength oscillations due to reflections within a layer of bauxite ore. We find that simply reducing the frequency of operation can significantly reduce these reflection effects.

The next step in this modelling is to carefully consider the connection between moisture content and the electromagnetic properties of the bauxite mixture. A large amount of effort and research has gone into the properties of grains and soils [1–3, 5, 6, 9, 10, 16]. This work is based on the original research of Maxwell [11], plus work by Wagner, Bruggeman, Clausius and Mossotti. Our model will then allow to connect ore porosity, saturation and height to signal strength and phase shift. One very interesting outcome will be to see whether the dependence of signal strength and phase shift upon moisture content is invertible or not.

## Acknowledgements

We are grateful to John and Hilary Ockendon (Mathematical Institute, University of Oxford) for conversations about solving Maxwell's equations with sufficient boundary conditions to find values for reflection coefficients, during work on a slab model for electromagnetic shielding at a subsequent Study Group in India that led directly to our approach here. Mark McGuinness is grateful to the MACSI group in the Department of Mathematics and Statistics for hosting the original Study Group that led to this work, and for their continued support.

## References


[1] T. L. Chelidze and Y. Gueguen, "Electrical spectroscopy of porous rocks: a review—I. Theoretical models", *Geophys. J. Int.* **137** (1999) 1–15; doi:10.1046/j.1365-246x.1999.00799.x.

[2] T. L. Chelidze, Y. Gueguen and C. Ruffet, "Electrical spectroscopy of porous rocks: a review—II. Experimental results and interpretation", *Geophys. J. Int.* **137** (1999) 16–34; doi:10.1046/j.1365-246x.1999.00800.x.

[3] Y. Chen and D. Or, "Geometrical factors and interfacial processes affecting complex dielectric permittivity of partially saturated porous media", *Water Resour. Res.* **42** (2006); doi:10.1029/2005WR004744.

[4] R. Collier, *Transmission lines: equivalent circuits, electromagnetic theory, and photons* (Cambridge University Press, Cambridge, 2013), Proquest Ebook Central. http://ebookcentral.proquest.com/lib/vuw/detail.action?docID=1113081.

[5] M. C. Dobson and F. T. Ulaby, "Active microwave soil moisture research", *IEEE Trans. Geosci. Remote Sens.* **24** (1986) 23–26; doi:10.1109/TGRS.1986.289585.

[6] T. Hanai, "Dielectric properties of emulsions", *Colloid Polymer Science* **177** (1961) 57–61; doi:10.1007/BF01521332.

[7] S. A. Kondrat'ev, V. I. Rostovtsev and I. I. Baksheeva, "Magnetization of minerals by radiation and heating and its prospects in mineral processing", *J. Mining Sci.* **52** (2016) 1183–1189; doi:10.1134/S1062739116061723.

[8] A. Kraszewski and S. Kulinski, "An improved microwave method of moisture content measurement and control Instrumentation", *IEEE Trans. Indust. Electron. Control Instrum.* **23** (1976) 364–370; doi:10.1109/TIECI.1976.351409.

[9] A. W. Kraszewski, S. Trabelsi and S. O. Nelson, "Broadband microwave wheat permittivity measurements in free space", *J. Microwave Power Electromagnetic Energy* **37** (2002) 41–54; doi:10.1080/08327823.2002.11688469.

[10] P. Lorrain, D. R. Corson and F. Lorrain, *Electromagnetic fields and waves*, 3rd edn (W.H. Freeman and Company, New York, 1988).

[11] J. C. Maxwell, *Lehrbuch der Elektricität und des Magnetismus*, 2 Bde (Springer, Berlin, 1883).

[12] M. McGuinness, S. Bohun, V. Cregan, W. T. Lee, J. Dewynne, G. O'Keeffe and T. Vo, "Measuring moisture in bauxite with microwaves", in: *Proceedings of the forum "math-for-industry" 2019 — Mathematics for the primary industries and the environment*, Volume 36 of Math. Industry (eds. R. McKibbin, G. Wake and O. Saeki) (Springer Nature, Singapore, 2021) 13–64; doi:10.1007/978-981-19-1154-5.

[13] C. E. Mullins, "Magnetic susceptibility of the soil and its significance in soil science: a review", *J. Soil Sci.* **23** (1977) 223–246; doi:10.1111/j.1365-2389.1977.tb02232.x.

[14] S. O. Nelson, "Models for the dielectric constants of cereal grains and soybeans", *J. Microwave Power Electromagnetic Energy* **22** (1987) 35–39.

[15] S. O. Nelson and S. Trabelsi, "Measurement of grain and seed microwave permittivity for moisture and density determination", in: *Proceedings of the IEEE SoutheastCon 2010 (SoutheastCon, 2010)* (ed. IEEE Web) (IEEE, Concord, NC, 2010) 463–466; doi:10.1109/SECON.2010.5453809.

[16] A. Sihvola, *Electromagnetic mixing formulas and applications*, Volume 47 of Electromagnetic Waves Series (Claricoats & Jull, The Institution of Engineering and Technology, London, UK, 1999); doi:10.1049/pbew047e.

[17] G. Taylor, R. A. Eggleton, L. D. Foster, D. B. Tilley, M. Le Gleuher and C. M. Morgan, "Nature of the Weipa Bauxite deposit Northern Australia", *Aust. J. Earth Sci.* **55**(S(1)) (2008) S45–S70; doi:10.1080/08120090802438241.

[18] S. Trabelsi and S. O. Nelson, "Free-space measurement of dielectric properties of cereal grain and oilseed at microwave frequencies", *Measurement Sci. Technol.* **14** (2003) 589–600; doi:10.1088/0957-0233/14/5/308.

[19] Y. Tu, L. Qin, E. Li, H. Ma, Y. Zhang, Y. Gao, C. Gao, J. Long, G. Guo, Y. Qiu, J. Li, H. Wu and X. Zhao, "Application of time-domain gating technique in water content measurement of gas–liquid two-phase flow", *Rev. Sci. Instrum.* **92** (2021) 094702; doi:10.1063/5.0055810.

[20] F. T. Ulaby, *Electromagnetics for engineers* (Pearson, Prentice-Hall, Upper Saddle River, NJ, 2005), Pearson International edition.

[21] S. A. A. Viana, "Microwave-based moisture measurement of Bauxite Ore on a Conveyor Belt", *Eng. Mining J. Features* (2013). https://www.e-mj.com/features/microwave-based-moisture-measurement-of-bauxite-ore-on-conveyor-belts/.

[22] L. Vojtech, M. Neruda and J. Hajek, "Planar material electromagnetic shielding efficiency derivation", *Int. J. Commun. Antenna Propagat.* **1** (2011) 21–28; https://www.researchgate.net/publication/297338460_Planar_materials_electromagnetic_shielding_efficiency_derivation.